PHYSICAL REVIEW B VOLUME 38, NUMBER 16 1 DECEMBER 1988

Nuclear-magnetic-double-resonance investigation of the dopant microstructure in hydrogenated amorphous silicon

J. B. Boyce and S. E. Ready
Xerox Palo Alto Research Center, Palo Alto, California 94304

(Received 1 August 1988)

Information on the local environment of dopants in compensated and singly doped amorphous Si has been obtained using NMR spin-echo double-resonance spectroscopy, a technique that is very sensitive to interatomic distance. It is found that there is a nonrandom local configuration around the dopants in these materials. In the compensated samples, almost half of the boron atoms have a phosphorus atom in the first-neighbor shell. This is higher than the value for a random distribution and indicates that there is significant clustering of the dopants in compensated material. In addition, the hydrogen atom is not directly bonded to either of these dopants. For the singly doped materials, the H-dopant structure is similar to that of the compensated samples for the P-doped samples but different for the B-doped material. For these, almost half of the B atoms have a hydrogen atom in the first-neighbor shell. This is to be contrasted with the P-doped samples where the H atoms are in second- or further-neighbor shells. Aspects of this local structure of P and B in hydrogenated amorphous Si are similar to those proposed for the dopant-H structures in hydrogen-passivated crystalline Si.

I. INTRODUCTION

Local bonding structures of dopants in crystalline and amorphous silicon are known to play a key role in determining the electrical properties of these semiconductors. The pertinent parameters are as follows: The number of neighbors (threefold or fourfold coordinated), the type of neighbors (Si, dopant, hydrogen), the local order (random or clustered), and the near-neighbor distances. The local environment of dopants in crystalline silicon has been determined to be fourfold coordinated substitutional sites with a local distortion of the surrounding Si tetrahedron. In contrast, the local environment in hydrogenated amorphous silicon (*a*-Si:H) is not known.[1] The fact that the doping efficiency is quite low suggests that the majority of the dopants are threefold coordinated rather than fourfold. A local structural probe, extended x-ray-absorption fine-structure (EXAFS) spectroscopy, has been used to study the dopant near-neighbor environment[2] for arsenic-doped *a*-Si:H. It supports the idea that the inactive dopants are threefold coordinated whereas the active dopants are fourfold. However, the fact that EXAFS is not sensitive to the light hydrogen atoms can cause substantial uncertainty in the conclusions about the local environment from these experiments.

Hydrogen most likely plays a significant role in determining the doping mechanism and efficiency, in addition to the Si coordination. In crystalline Si, it is known that hydrogen passivates acceptor[3-7] and donor[7,8] states. Although the precise mechanisms of acceptor and donor passivation have not, as yet, been settled, the various models that are consistent with the available data involve local bonding configurations with the hydrogen atom near the dopant atoms.

In contrast to x-ray structural probes such as EXAFS and diffraction, NMR is sensitive to hydrogen. In addition, double-resonance techniques exist that provide relative distance information. Here we describe the results of NMR double-resonance experiments, namely, spin-echo double resonance, which was used to probe the local environment around the dopants in singly doped and compensated *a*-Si (Refs. 9 and 10). These double-resonance studies differ from single-resonance studies of the dopant atoms themselves in that the double resonance yields direct information on the relative location of a particular pair of atoms spectroscopically selected by the two NMR frequencies used. The single-resonance experiments must contend with the contributions of all the atoms present in the material. Nonetheless, significant structural information can and has been obtained from these experiments. For example, in *p*-type material, boron has been reported[11,12] to reside in two distinct sites: one consisting largely of axially symmetric BSi_3 structures and another consisting of $BHSi_2$ sites with the B-H distance somewhat relaxed. In the analysis of P NMR in *n*-type *a*-Si, the majority of P was found to reside in threefold coordinated structures.[13,14] For the fourfold coordinated P atoms, spin-echo-decay data indicated that P is about 5 Å from hydrogenated surfaces.

In this paper, we report on the local structure of dopants in hydrogenated amorphous silicon as determined by the NMR spin-echo double-resonance (SEDOR) technique. Section II describes the SEDOR technique used, and Sec. III presents the experimental details and single NMR results. Section IV presents the SEDOR results both on known structural standards used to calibrate the spectrometer and on the *a*-Si samples. Section V discusses these data and contrasts them with other NMR measurements. Section VI presents the conclusions.

II. EXPERIMENTAL TECHNIQUE

NMR spin-echo double resonance[15,16] is a technique by which one can selectively measure the size of the local magnetic field produced by the nucleus of a specific species, J, at the location of another species, I. As a result, this yields information on the relative spatial position of I and J since the dipolar coupling varies rapidly with distance as $1/r^3$. Standard single-resonance NMR techniques measure the total local field at the site of the resonating nucleus, due to all the other nuclear spins in the sample via the NMR linewidth. For a multicomponent sample, the individual component interactions are not determined, only their sum. SEDOR, on the other hand, measures only a selected portion of the local field. The spectrometer can be tuned to select out a particular pair of spins, I and J, and determine their pair interactions separate from the other interactions in a multielement sample, i.e., independent of the I-I, I-K, . . . ,interactions. One thereby acquires information on the relative spatial relationship of the I and J spins.

The SEDOR measurements are performed using a standard spin-echo[17] pulse sequence (P_1-τ-P_2) applied to a receiver coil tuned to the I-spin resonance while also applying a third pulse, P_3, at another radio frequency to a second NMR coil tuned to the J-spin resonance. The I-spin echo occurs at a time τ after the second pulse P_2 or at $t=2\tau$ after the first pulse P_1. In the simplest case, P_1 is a 90° pulse that tips the I spins from their alignment along the z axis, the direction of the external applied magnetic field, H_0, down into the x-y plane, and P_2 is a 180° pulse. We consider the case where the spin-lattice relaxation time, T_1, is infinite and so can be ignored. This is a valid assumption in the systems studied here as shown below in Sec. III. Following the 90° pulse, the I spins precess in the x-y plane at the Larmor frequency, $\omega_I=\gamma_I H_0$, where γ_I is the I-spin gyromagnetic ratio. There is a spread of I-spin resonance frequencies, $\Delta\omega_I$, due to the interactions with the other spins in the system, due to a distribution in chemical shifts, and due to a spread in the external applied field over the sample. This width in resonance frequencies results in a width to the NMR resonance signal and a corresponding dephasing of the spins as they precess about the z axis at somewhat different frequencies with a dephasing time of $T_2^* \approx 1/\Delta\omega_I$. The signal induced in the receiver coil, the free induction decay (FID), is proportional to the net macroscopic nuclear moment and so decays with time constant T_2^*, i.e.,

$$S(t)=S_0\exp(-t/T_2^*)\ .$$

This dephasing rate, $1/T_2^*$, consists of two parts, a homogeneous component, $1/T_2$, and an inhomogeneous part due to a distribution of magnetic fields over the sample, different chemical shifts, etc. As a result, $1/T_2^* \geq 1/T_2$. The portion of this decay due to the inhomogeneous broadening of the line will refocus in the spin echo, whereas the homogeneous decay is irreversible. So the echo amplitude, which peaks at $t=2\tau$, will decay with time as $\exp(-2\tau/T_2)$, slower than the free-induction decay of $\exp(-t/T_2^*)$. For the moment we ignore the effects of T_2, i.e., assume that it is infinite.

Consider an ensemble of identical I spins that are each coupled to one J spin. For simplicity, take $J=\frac{1}{2}$. For the double-resonance experiments an additional rf pulse, P_3, is applied simultaneously with P_2, on a second coil at the resonance frequency of the J spins, ω_J. For a 180° pulse, the J spins are flipped from pointing up (down) along the z axis to pointing down (up). This produces a modification of the local magnetic field seen by a nearby I spin, resulting in a change in the precession frequency of the affected I spins during the second τ time interval. As a result, all the I spins no longer rephase completely at $t=2\tau$ to form the echo signal. The extra phase is $\delta\theta=\delta\omega_d\tau$, where $\delta\omega_d$ represents the change in the dipolar field due to the flip of the J spin. The echo amplitude, S, is reduced by this phase factor

$$S(2\tau)=S_0\cos(\delta\omega_d\tau)\ . \tag{1}$$

If the pulse P_3 is imperfect due to a distribution in rf field strength over the sample, due to finite rise and fall times, due to a deviation from 180°, or due to having a frequency different from the J-spin resonance frequency, then the *change* in the echo signal is reduced by a factor of α which is ≤ 1:

$$\Delta S(2\tau)=(S_0-S)/S_0=\alpha[1-\cos(\delta\omega_d\tau)]\ . \tag{2}$$

The pulse width and frequency dependence of α goes as

$$\alpha\approx A_J\sin^2(\Omega_J t_w/2)(\omega_1^2/\Omega_J^2)\ , \tag{3}$$

with

$$\Omega_J^2=[\omega_1^2+(\omega-\omega_J)^2]\ , \tag{4}$$

where ω is the frequency of the applied J-spin pulse, ω_1 and t_w are the amplitude in frequency units and pulse width of the rf field applied to the J spins ($\omega_1 t_w=\pi$ for a 180° pulse), and A_J is the isotopic abundance of the selected J spin. For a perfect 180° P_3 pulse on resonance and for $A_J=1$, $\alpha=1$. For P_3 far from the J-spin resonance frequency, or for a 360° P_3 pulse, $\alpha=0$ and no SEDOR destruction occurs. Values of α found in our experiments were between 0.85 and 1. The small reduction from 1 was due to imperfect pulses since the SEDOR pulse was adjusted to be on resonance and to yield maximum destruction, i.e., $\omega_1 t_w \approx \pi$.

Expressions (1) through (4) apply for identical I spins coupled to a single J spin with $J=\frac{1}{2}$. If the I spins are coupled to N_J spins instead of just one, then the SEDOR signal is given by

$$S=S_0\prod_j\{1-\alpha_j[1-\cos(\delta\omega_j\tau)]\}\ , \tag{5}$$

where the product is over the N_J I-J couplings with α_j given by Eq. (3) and

$$\delta\omega_j^2\sim\gamma_I^2\gamma_J^2\hbar^2(1-3\cos^2\theta_j)^2/r_j^6 \tag{6}$$

for dipolar coupling. θ_j is the angle between the vector connecting I and J and the applied magnetic field, the z axis. Here we ignore any indirect scalar or indirect dipolar coupling which may be appropriate in many systems but appear to be insignificant for the systems studied here. For a powder sample, Eqs. (5) and (6) must be averaged over the powder distribution in θ_j.

Equation (5) is unwieldy and can only be used to extract local structural information in simple cases.[18] It is convenient for the analysis here to use an approximation to Eq. (15). Consider Eqs. (1) and (2) with a Gaussian distribution in $\delta\omega_d$. Such a distribution is a reasonable approximation for the systems studied here since there will be a range of *I*-*J* couplings due to the powder average in Eq. (6), due to a distribution in *I*-*J* spin configurations, and so on. If we then average $\delta\omega_d$ over a Gaussian distribution in values, the resulting expression can be approximated by the relation

$$\Delta S(2\tau)=(S_0-S)/S_0\approx\alpha[1-\exp(-2\Delta\omega_{IJ}^2\tau^2)]\ , \quad (7)$$

where $\Delta\omega_{IJ}^2$ is the second moment of the interaction between the *I* and *J* spins. The structural information is contained in this coupling constant according to

$$\Delta\omega_{IJ}^2\approx[\gamma_I^2\gamma_J^2\hbar^2/5](N_J/r^6)\ , \quad (8)$$

where r is the distance between the *I* spin and the shell of N_J *J* spins. If there are more than one shell of *J* spins that are coupled to the *I* spin, then (N_J/r^6) is replaced by $(\sum_J 1/r_j^6)$, where the sum is over all the *J* spins located at a distance r_j from the *I* spin. Equations (7) and (8) are approximations to the more exact expressions of the previous paragraph but are rigorously equivalent to them in the short-time limit, i.e., $\Delta\omega_{IJ}\tau\ll 1$. In any case, the decay of the signal amplitude with time is seen to be very sensitive to the distance between the two participating spins.

Equations (1)–(8) assume that all the resonating *I* spins are essentially equivalent as far as their coupling to the *J* spins is concerned. If there are more than one inequivalent site with significantly different environments, such as *I* spins coupled to *J*-spin first neighbors and *I* spins with no *J*-spin neighbors, then two or more expressions of the type of Eq. (7) are appropriate. For the two-environment case, Eq. (7) becomes

$$\Delta S(2\tau)=(S_0-S)/S_0\approx\alpha[1-f_1\exp(-2\Delta\omega_1^2\tau^2)-f_2\exp(-2\Delta\omega_2^2\tau^2)]\ , \quad (9)$$

where $(f_1+f_2)=1$ with f_1 and f_2 being the fractions of the *I* spins in environments 1 and 2 with coupling constants $\Delta\omega_1^2$ and $\Delta\omega_2^2$, respectively. This is the expression that will be used here to analyze the data in the amorphous materials where a large number of *I*-spin environments are expected but the signal-to-noise ratio obtainable does not warrant a more complex analysis. In this case the two coupling constants are approximations to the true situation. Nonetheless, due to the rapid distance dependence of the SEDOR, the near-neighbor couplings dominate the spectrum. This provides a substantial reduction in the number of possible configurations. The SEDOR is sensitive only to those configurations that are different in their near-neighbor arrangement. $\Delta\omega_1^2$ can be considered as due to first- or second-neighbor coupling and $\Delta\omega_2^2$ as a mean coupling due to second and further neighbors. Equation (9) thereby provides a good representation of the data with the major structural information contained in the larger coupling constant, $\Delta\omega_1^2$.

The preceding expressions were obtained under the assumptions that T_1 and T_2 are infinite, i.e., much longer than $1/\delta\omega_d$. This is true for T_1, as will be discussed later in Sec. III. However, it is not necessarily true for T_2. The T_2 decay of the *I* spins themselves does not enter the SEDOR decay since it only produces a change in the echo intensity with τ and is removed in the ratio of $S(2\tau)$ to $S_0(2\tau)$, the SEDOR signal. It will mainly effect the range of τ over which the SEDOR decay can be measured with a reasonable signal-to-noise ratio, i.e., for τ's up to a couple of *I*-spin T_2's. Beyond this point, the *I*-spin echo is lost in the noise. The spin-spin coupling of the *J* spin effects their orientation *during* the SEDOR measurements. In simple terms, the *J* spin that is flipped down by the 180° pulse does not stay down during the SEDOR measurements. Rather it precesses in the field due to the coupling to other *J* spins and can be flipped back up. But since there is an ensemble of such interactions, the major effect is to give a finite width to the *J*-spin resonance. For the weak *J*-*J* coupling of the dopants this presents no difficulty. However, the *H* spins are more strongly coupled to one another due to their larger magnetic moment and higher density, and so the dopant-H SEDOR results could be effected. The *J*-spin pulse amplitude has to be large enough to cover the entire *J*-spin line, i.e., $\omega_{IJ}>J$-spin line width. Some of the changes in the SEDOR decay due to a large *J*-spin width will be accounted for by an increase in α since not all the *J* spins will be flipped if the line is broad. The strongest dopant-H coupling, $\Delta\omega_1^2$, is the least effected, and so we will only draw conclusions based on it. The weaker dopant-H coupling of Eq. (9), $\Delta\omega_2^2$, represents some average that could be modified by the H-H coupling and so its physical significance cannot easily by determined.

III. EXPERIMENTAL DETAILS

A. Experimental arrangement

The single NMR and SEDOR measurements were performed on P- and/or B-doped *a*-Si:H as well as two structural standards, BP and BPO_4, which were used to calibrate the SEDOR spectrometer. All the data were taken at room temperature in a dc magnetic field of 74 kG for which the resonance frequencies are $\omega(P)/2\pi=128$ MHz, $\omega(B)/2\pi=101$ MHz, and $\omega(H)/2\pi=315$ MHz. For the SEDOR measurements, a standard spin-echo pulse sequence $(P_1-\tau-P_2)$ was applied to a central receiver coil. The third pulse was applied at another radio frequency to a second coil in a crossed-coil configuration. The central coil excites the *I* spins at their resonance frequency to produce a rephasing of these spins at a time 2τ from the initial rf pulse, P_1. The rephasing of the spins produces an echo signal of amplitude $S_0(2\tau)$ and is picked up by the same central coil. A 90°-τ-180° pulse sequence was used for the nuclei that were not affected by quadrupole interactions, i.e., phosphorus ($I=\frac{1}{2}$ and, therefore, no quadrupole moment) and boron ($I=\frac{3}{2}$) in cubic environments. For B in the a-Si, quadrupole interactions split the various spin levels. In this case, the boron echo signal was maximized with a quadrupole echo sequence, namely, a 90°-τ-(45°-90°)$_{90}$ sequence [(45°-90°)$_{90}$ denotes a pulse between 45° and 90°, inclusive, with a 90° phase shift]. A second echo pulse sequence is then applied with the addition of the third rf pulse applied simultaneously with P_2, on the crossed coil at the resonance frequency of the J spins. A 180° P_3 pulse was used. The reduced echo amplitude, $S(2\tau)$, was then recorded and the ratio $S(2\tau)/S_0(2\tau)$ calculated. This ratio was measured as a function of τ to give the SEDOR decay. The I-spin pulse was large ($\omega_1/2\pi \approx 120$ kHz) while the J-spin pulse was about 3–4 times smaller due to its larger crossed-coil volume. This was large enough to cover the P line and sufficient to cover most of the H line.

B. Samples

All the a-Si samples were grown by glow discharge from silane gas onto substrates heated to 230 °C. 1% PH_3 and/or 1% B_2H_6 dopant gases were added to the SiH_4 gas. The plasma was produced by an rf excitation of about 0.07 W/cm^2. The resulting amounts of B and P are approximately 0.5 at. % for the singly doped samples and 2.0 at. % for the compensated samples as determined by secondary ion microscopy and by the NMR signal intensity, using BP as a standard. The amount of H, determined by NMR, is about 10 at. %. The pertinent NMR results of the samples studied most extensively here are listed in Table I. Similarly prepared samples were also measured to verify the results but with fewer data points and poorer signal-to-noise ratios. The discussion here will emphasize these extensively studied samples and reference to the other samples will be made only where their results qualify the conclusions. Before discussing the SEDOR results, we summarize the single resonance data on the H and the dopants.[10]

C. Hydrogen NMR

The hydrogen NMR line widths obtained are typical of undoped materials prepared in the same manner and have been interpreted[19–22] as arising from a clustered phase (broad line) and a dilute phase (narrow line). The narrow line has a full width at half maximum (FWHM) of about 3 kHz and contains about 3 at. % H. The broad line has a FWHM of about 25 kHz and contains the remainder of the H. No substantial difference in the H content or distribution due to the doping is apparent, except for a somewhat smaller fraction of the H contributing to the narrow line for the B-doped material ($\approx$2 at. % versus a more typical value of 3 at. %). Other studies have observed increases in the H content with doping,[14,19] but this does not appear to be the case for these samples where the other parameters that strongly effect the H content, like substrate temperature and gas composition, were kept the same. Also, using multiple-quantum NMR (Refs. 23 and 24), differences have been observed in the H cluster size of the clustered phase as the dopant level is changed, but these small changes are beyond the sensitivity of the single-resonance technique used here. In addition, the values of the H spin-lattice relaxation time, T_1, are similar to those in the much-studied[20,25–29] undoped a-Si, and the relaxation process is due to the presence of a small number of H_2 molecules trapped in voids in the material (about 1–3 % of the H) (Refs. 30 and 31).

D. Phosphorus NMR

The phosphorus spin-echo amplitude for both the compensated and the n-type samples decays exponentially with increasing τ over more than an order of magnitude, yielding a long T_2 of approximately 1.1 msec. This long T_2 and single exponential behavior are both consistent with a dilute-spin system. If the 2 at. % P of the compensated sample is placed on a simple cubic lattice, then T_2 can readily by estimated from the Van Vleck second moment[32] of the line, $\Delta\omega^2$, as $1/T_2 \approx (\Delta\omega^2)^{1/2}$. For 2 at. % P and the a-Si density, the mean spacing of the P is about 10 Å, and the calculated T_2 due to P-P dipolar interactions is 4 msec. Such a calculation overestimates T_2. A spread in distances appropriate for amorphous systems and a random rather than an ordered distribution will substantially lower T_2 due to its strong $1/r^3$ distance dependence. The measured value of 1.1 msec can, therefore, be consistent with P-P dipolar interactions and, in fact, is in agreement with a calculation[13] using a random distribution of P. The dipolar interactions with ^{29}Si are too weak to account for the observed T_2. A similar cubic-lattice estimate yields T_2 (P-^{29}Si) $\approx$20 msec. H

TABLE I. Pertinent NMR results of the most extensively studied doped a-Si samples.

Sample	Dopant conc. (at. %)	H conc. (at. %)	H T_1 (sec)	P T_1 (sec)	B T_1 (sec)	P T_2 (msec)
Compensated a-Si:(H,B,P)	2% P 2% B	13	2.8	1100	143	1.15
P-doped a-Si:(H,P)	0.5% P	10	1.8	90		1.10
B-doped a-Si:(H,B)	0.5% B	10	1.4		7	

could account for the measured value, but a previous study involving the removal of H by annealing concluded that P-P interactions dominated the P-echo decay.[13]

It is interesting to note that the same value of T_2 is obtained for the singly doped sample despite the fact that the total phosphorus concentrations in the two samples differ by a factor of 4. This fact may indicate that the phosphorus resides in regions of the material where the P concentration remains constant. Nonetheless, it is even more interesting that P interactions alone can account for the P T_2, despite the fact that a much higher concentration of H is also present in the sample. Since P is dilute and H has a large magnetic moment and is more concentrated, one would expect that the P-H dipolar interaction should dominate the P T_2. The fact that this is not the case implies that the P resides in regions of the sample where the H is dilute, possibly the dilute phase.

A previous study has observed 20% of the total P to be fourfold coordinated P and exhibit a rapid echo decay ($T_2 \leq 200$ μsec) due to close association to H clusters.[13,14] Our echo results show no indication of such a large and rapid decay.[10] All of the P contributes to the echo since the echo amplitude measured down to $\tau = 25$ μsec and extrapolate to $t=0$ agrees with the FID amplitude. Although the decay is not a perfect exponential, a component of order 20% with a different T_2 is not present. It appears, however, that this fourfold coordinated P is metastable.[14] It requires a dark anneal to be present and can be eliminated by light soaking. Our samples were exposed to light so that any metastable, fourfold P that might be present is eliminated.

The phosphorus free-induction decay is significantly faster ($T_2^* \approx 20$ μsec) than the echo decay indicating that the primary source of resonance broadening is inhomogeneous in nature. It is most likely due to a distribution of chemical shifts and chemical-shift anisotropy, both of which refocus in the echo.

The spin lattice relaxation time (T_1) of the phosphorus is an order of magnitude larger for the compensated sample (1100 sec) than for the *n*-type sample (90 sec). Such a variation is expected if the dominant relaxation mechanism is interactions with conduction electrons. The recently observed[14] frequency dependence of T_1 indicates that there is a component due to disorder modes.[33,34] The relaxation may then be due to a combination of conduction electrons and disorder modes. In any event, it is weak and gives rise to very long T_1's, thereby making P NMR measurements difficult.

E. Boron NMR

The boron echo decays for both the compensated and *p*-type samples were fast and highly nonexponential, indicating a substantial quadrupolar coupling. Also due to the large linewidths, the B linewidth parameters were determined using quadrupolar echos.

In the compensated sample, three resonance lines could be distinguished in the echo spectrum: one very broad line (FWHM > 120 kHz, $T_2^* \approx 3$ μsec) due to half the B, one moderately broad resonance (FWHM = 27 kHz, $T_2^* = 12$ μsec) accounting for one quarter of the signal, and an additional narrow line (< 2 kHz, $T_2^* >$ 180 μsec) due to $\frac{1}{4}$ of the B. The very fast decay could only be recorded using a spin echo due to its short decay time of 3 μsec compared with the longer time of 8 μsec for the receiver system to recover from the large overload of the rf pulses. The value for the width of the very broad line is a lower limit due to the limited spectral width (120 kHz) of the applied rf field. We can only give an upper limit to the width of the narrow line due to signal-to-noise limitations at times far from the echo peak. For the *p*-type sample, the boron resonance exhibits two resonance lines: one very broad line (FWHM > 220 kHz) corresponding to a very fast decay (1.2 μsec), similar to the 3 μsec decay in the compensated sample, and one moderately broad line (FWHM = 13 kHz, $T_2^* = 25$ μsec).

The linewidth of the boron resonance in *a*-Si has been shown[11] to be inversely proportional to the applied magnetic field, indicating that second-order quadrupole interaction is the primary source of line broadening. The moderately broad lines in both samples compare well with data from previous studies[11,12] of *a*-Si:(H,B) and borate minerals in threefold coordinated sites.[35] As a result, the moderately broad lines can be identified as due to threefold coordinated boron. The very broad line arises from boron residing in regions of the material with very large electric field gradients due to larger distortions than for the threefold coordinated sites of the borate minerals. One can only speculate that these may be due to highly distorted BSi_3 and/orBSi_2H units.

The width of the narrow boron line, as seen only in the compensated sample, is quite comparable to the linewidth of tetrahedrally coordinated boron (< 2 kHz) measured in crystalline silicon.[36] Thus we attribute this resonance to fourfold coordinated boron atoms. This component corresponds to about $\frac{1}{4}$ of the B or 0.5 at. %. This is very large considering the fact that the doping efficiency is quite low in *a*-Si. However, the doping efficiency in compensated samples can be two orders of magnitude larger than in singly doped material.[37] But as will be seen later, about half of the B have a P near neighbor. So these fourfold coordinted B atoms, only observed in the compensated material, most likely consist of B with three Si and one P, i.e., $BPSi_3$ units.

IV. SEDOR EXPERIMENTAL RESULTS

A. Structural standards

The B echos in BP and BPO_4 were measured as a function of time, τ, while applying the double resonance pulse to the P to obtain the SEDOR decay. The amplitude of the B echos with a pulse spacing of τ were measured at $t=2\tau$ both without, $S_0(2\tau)$, and with, $S(2\tau)$, the P_3 destruction pulse. The ratio $S(2\tau)/S_0(2\tau)$ was obtained for a number of τ's to give the SEDOR decay. A B-P SEDOR signal decay in BP is shown in Fig. 1. The notation that we will use in labeling these results is that the first atom mentioned, the B, is the *I* spin, the species whose echo is observed. The second atom listed, the P, is the *J* spin, the one flipped to cause the *I*-spin decay. In Fig. 1, the line through the data points represents a fit us-

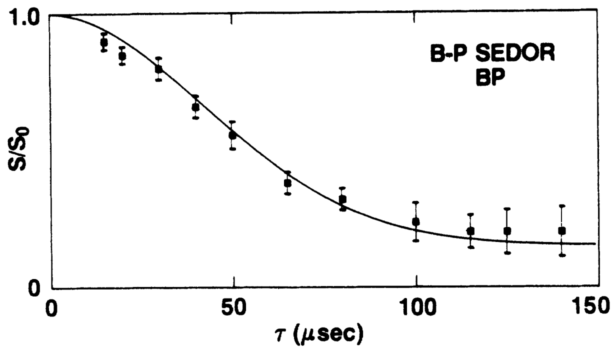

FIG. 1. B-P SEDOR decay for the structural standard BP. The curve through the data points is a one Gaussian fit to the data that yields the B-P first-neighbor environment in agreement with the known structure.

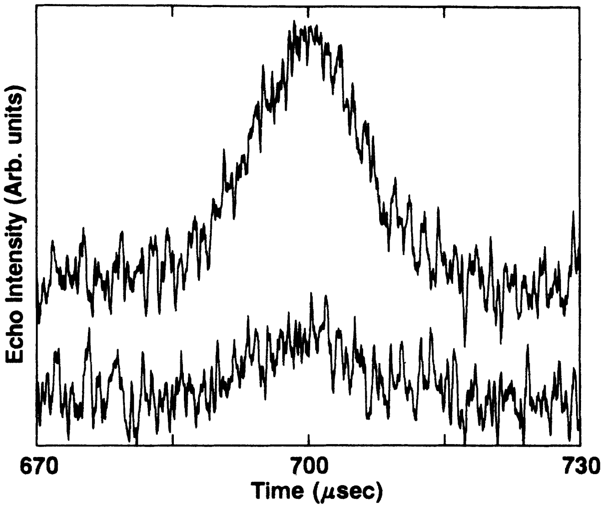

FIG. 2. Spin echos for phosphorus in singly doped a-Si:(H,P). The bottom trace shows the destruction in this echo amplitude due to flipping the hydrogen atoms. The echo τ is 350 μsec; 45 echos were averaged for these curves, and the $t=0$ of the time axis is taken at the first pulse, P_1, of the echo sequence.

ing a single Gaussian of the form in Eq. (7). The obtained B-P coupling constant is

$$(\Delta\omega^2)^{1/2}/2\pi \approx 1.64 \text{ kHz} .$$

The B-P spacing and number of near neighbors obtained from this decay, using Eq. (8), are within 4% of the known structural parameters of the zinc-blende structure of BP (1.96 Å and 4 P neighbors). If the 12 P third neighbors at 4.94 Å are added, little change in the fit is observed, consistent with the strong distance dependence of the SEDOR.

From Fig. 1, it is evident that S/S_0 approaches 0.15 and not zero as $\tau \rightarrow \infty$. This provides a determination of $\alpha \approx 0.85$. P has an isotopic abundance of 100%, and the P pulse was optimized for this measurement, that is to say, its frequency was adjusted to be on resonance and its amplitude and width set for a 180° pulse. As a result, the deviation of α from 1 is due to the known imperfections in the SEDOR pulse, namely, inhomogeneities over the sample and finite rise time, fall time, and width. This provides a calibration of the spectrometer for the B-P SEDOR measurements. The tests using BPO_4 provided similar results. The determined B-P coupling constant of

$$(\Delta\omega^2)^{1/2}2\pi \approx 0.66 \text{ kHz}$$

yields 4 B-P pairs with a spacing of 2.76 Å, in agreement with the known structure having a B-P spacing of 2.73 Å. For the B-H SEDOR, BH_3-NH_3 was used to test the high-frequency (315 MHz) crossed coil for the H pulse and to calibrate the spectrometer for these experiments.

B. Amorphous materials

For all the amorphous materials, the SEDOR pulse, P_3, was applied at the hydrogen NMR frequency, giving information on the B-H and P-H local structure. In addition, for the compensated material, the echo pulses were applied at the B NMR frequency while P_3 was applied at the P frequency, giving B-P local structural information. Due to the small number of dopant atoms in the samples, the I-spin-echo signal has a poor signal-to-noise ratio. As a result, averaging was employed and typically 100 echos were summed at each time τ to get the SEDOR decay. Representative P echos, both without and with the P_3 destruction pulse, are shown for a-Si:(H,P) in Fig. 2. $\tau = 350$ μsec $< T_2/2 = 550$ μsec and 45 averages were used. The reduction in the echo amplitude due to P_3 is evident. In addition, the finite signal-to-noise ratio that limits the precision of the structural determination is apparent.

1. Compensated sample

The SEDOR signal decay versus τ for the B-P in a-Si:(H,B,P) is shown in Fig. 3. The line through the data points represents a fit using two Gaussians of the form in Eq. (9) and is discussed later. The other curves represent the decays for three other structural models. In all these model calculations, we used $\alpha = 0.85$, as determined above. Curve A is the clustered case where all B atoms are bonded to a P atom at a distance of 1.96 Å appropriate for BP. Curve B corresponds to an approximation for a random distribution of the B and P atoms. This distribution consists of 8% of the B having one P first neighbor at 1.96 Å. (8% = 2 at. % times four first neighbors.) This 8% of the total B echo, therefore, has a rapid SEDOR decay. In addition, 24% of the B have a P in the second-neighbor shells at about 3.5 Å and have a slower decay. And so on for the further neighbor B-P pairs. Only the first part of the decay is shown in Fig. 3. Curve C corresponds to the maximum possible B-P mean separation of 8.6 Å by placing the 2 at. % B and 2 at. % P atoms in a CsCl-type structure. None of these models fit the data, although the data are between the fully clustered and totally random cases. Of note here is the rapid initial decay in the data, indicating, via Eq. (7), a short B-P distance in the compensated sample.

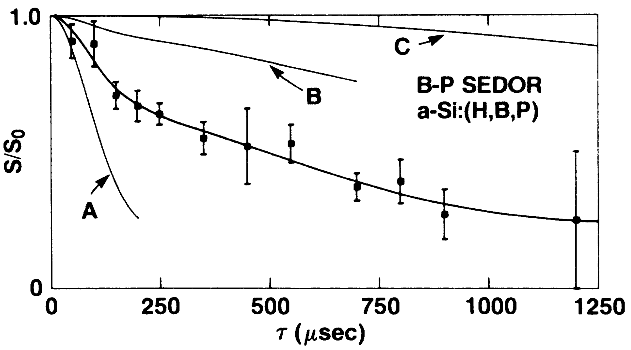

FIG. 3. The B-P SEDOR decay for compensated *a*-Si. The curve through the data points is a two Gaussian fit as described in the text, with the results listed in Table II. Curve *A* is for a totally clustered situation, i.e., each B bonded to a P. Curve *B* is for a random distribution of B-P pairs, and Curve *C* is for a CsCl arrangement of the 2 at. % B and P. None of these three situations is seen to reproduce the data.

This is confirmed by the two Gaussian fit to the data, shown as the solid line through the data points. The two inequivalent B sites that fit the data are 40% of the B with a B-P coupling constant of

$$(\Delta\omega_1^2)^{1/2}/2\pi \approx 0.8 \text{ kHz}$$

and the remainder of the B with a B-P coupling constant of

$$(\Delta\omega_2^2)^{1/2}/2\pi \approx 65 \text{ Hz} .$$

These coupling constants correspond, via Eq. (8), to 40% of the B with a P atom at 2.1 Å and 60% of the B with P at a mean distance of about 3.8 Å. These results are summarized in Table II. The distances from the dopant, *I*-spin atom to the nearest neighboring *J*-spin atom is given by r_1 along with the associated percentage of dopant, *I*-spin atoms and with this distance. The value r_2 can be interpreted as a characteristic distance derived from an average value of the coupling constant for all other dopant sites not included in r_1. It is not necessarily to be taken as a specific B-P distance for a second or third neighbor. Rather it means that 60% of the B atoms have P atoms further than 2.1 Å and closer to 3.8 Å. Also shown in Table II are the values expected if the bonding were totally random and if the selected pair of atoms were clustered, e.g., all B bonded to a P. The first site indicates that 40% of the B and P are clustered since their B-P distance is close to that in BP. It should also be mentioned that an α of 0.85 is found, consistent with that determined from the BP standard.

Similar measurements were performed on this sample flipping the H atoms instead of the P atoms. This B-H SEDOR decay curve is shown in Fig. 4. Curve *A* is the decay expected if all the B have a H atom bonded at 1.4 Å. This value is one expected for direct B—H bonds in *a*-Si since r(B—H)=1.2Å and 1.4 Å in B_2H_6 and r(Si—H)=1.4 Å. Curve *B* is the first part of the decay for a random distribution with 34% of the B having a H first neighbor at 1.4 Å [$34\% = 4 \text{ neighbors} \times 13$ at. % $\text{H} \times (1-0.13)^3$]. Neither of these curves follow the data since a hydrogen atom in the first-neighbor shell of the B causes too rapid a decay. From the data we see that no significant fraction of the B atoms can have a H directly bonded to them. The two Gaussian fit to the data, the solid line through the data points in Fig. 4, confirms this. The determined value of α is about 0.85. The results, listed in Table II, show that the shortest distance consistent with the data is 2.5 Å, closer to a second-neighbor B-H distance.

A third SEDOR measurement was performed on this compensated sample, namely, a P-H SEDOR. The decay of the P echo versus τ due to flipping the H atoms is

TABLE II. Phosphorus and boron SEDOR results for compensated *a*-Si:(H,B,P) and samples singly doped with P and B. The two-peak experimental results are shown, with Fract. being the fraction of the atom pairs with the given distance. The uncertainties in the experimental results are about ±0.3 Å in distance and ±15% in the fraction of pairs at a given distance. For comparison, the expected near-neighbor arrangements for a random distribution and for a clustered local environment are also given. Both of these cases have the same distances.

		Experiment peak 1		Experiment peak 2		Random and clustered cases		
Sample	SEDOR pair	r_1 (Å)	Fract. (%)	r_2 (Å)	Fract. (%)	r (Å)	Rand. fract.	Clust. fract.
a-Si:(H,B,P)	B-P	2.1	40	3.8	60	1.96	8	100
2 at. % P								
2 at. % B	B-H	2.5	40	3.7	60	≈1.4	43	100
13 at. % H	P-H	2.6	50	4.3	50	1.42	43	100
a-Si:(H,P)								
0.5 at. % P	P-H	2.6	53	4.1	47	1.42	35	100
10 at. % H								
a-Si:(H,B)								
0.5 at. % B	B-H	1.6	40	3.1	60	≈1.4	35	100
10 at. % H								

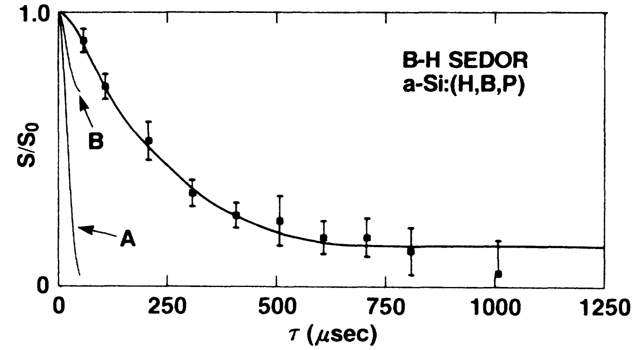

FIG. 4. The B-H SEDOR decay for compensated *a*-Si. The curve through the data points is a two Gaussian fit as described in the text, with the results listed in Table II. Curve *A* is for a totally clustered situation, i.e., each B bonded to a H, and Curve *B* is for a random distribution of B-H pairs. Neither of these situations reproduces the data.

shown in Fig. 5. The solid line is a two Gaussian fit to the data using Eq. (9), with a determined value of $\alpha \approx 1$. The extracted distances are given in Table II, and the conclusions are similar to those for B-H: no significant fraction of the P atoms have a H bonded directly to them but rather half have an H at a distance comparable to a second-neighbor spacing.

2. Singly doped samples

The SEDOR signal decay versus τ for the P-H in *a*-Si:(H,P) is similar to that for the compensated sample shown in Fig. 5. The two inequivalent P sites that fit the data are about 53% of the P with an H atom at 2.6 Å and the remainder of the P with H at a mean distance of about 4.1 Å. These results are listed in Table II. Again, the H is not directly bonded to a measurable fraction of the P but rather close to 53% have a H in roughly the second-neighbor shell.

The dopant-H SEDOR of Figs. 4 and 5 is to be contrasted with the B-H SEDOR in singly doped *a*-Si:(H,B), shown in Fig. 6. Unlike these other curves, Fig. 6 shows a rapid initial decay, indicative of a short B-H distance.

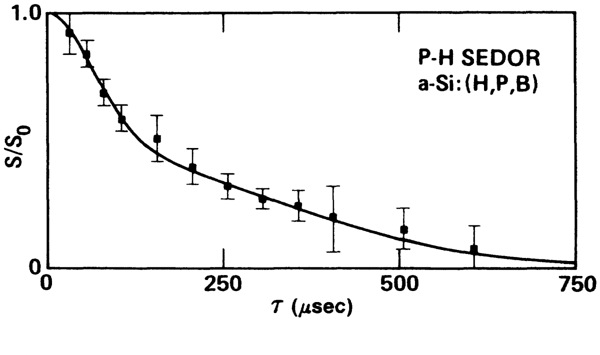

FIG. 5. The P-H SEDOR decay for compensated *a*-Si. The curve through the data points is a two Gaussian fit as described in the text, with the results listed in Table II.

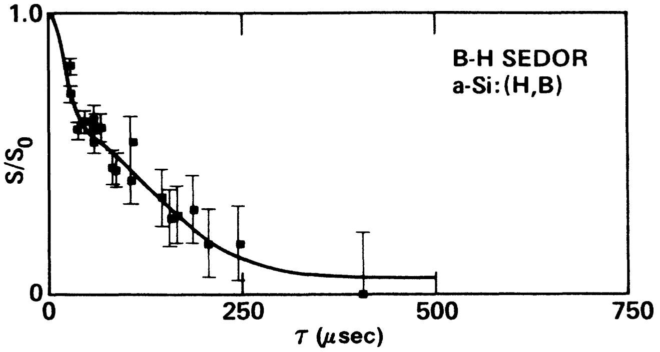

FIG. 6. The B-H SEDOR decay for *p*-type *a*-Si. The curve through the data points is a two Gaussian fit as described in the text, with the results listed in Table II. The rapid initial decay indicates that a significant fraction of the B atoms have a H atom at a short first-neighbor distance.

The two Gaussian fit, the solid line in the figure, yields the distances in Table II. 40% of the B atoms have a H atom at about 1.6 Å, very close to typical B-H distances in boranes. The remainder of the B have H neighbors further away at a mean distance of 3.1 Å. These results show that the H is bonded very close to about half of the dopant atoms (very likely direct bonding) in *p*-doped *a*-Si but not in *n*-doped or compensated material. It should be mentioned that the precise fraction of the H that is bonded to the B varies somewhat from sample to sample. Another B-doped sample prepared under similar conditions gave about 25% of the B with a H in the first-neighbor shell, rather than 40%. Nonetheless, the basic conclusions, namely, a significant fraction of the B having a H in the first-neighbor shell, is confirmed.

Before concluding this section, we should mention the tests performed on the analysis of the data using the approximation of Eq. (9). We analyzed a more rigorous model appropriate for a random distribution of dopant and hydrogen atoms. We approximated the local atomic configuration around the dopant with that of crystalline silicon, using the appropriate dopant-dopant and dopant-hydrogen distances known from standards. The probability that a certain atomic arrangement exists within the first four shells was calculated using a random distribution. We then calculated the expected SEDOR decay as a superposition of effective decays associated with each possible arrangement using a powder averaged form of Eq. (5). The results confirmed the analysis using the simple expressions. These tests implied that the approximate expression, Eq. (9), provides an adequate description of the data.

V. DISCUSSION

The single-resonance results on the P and B that are pertinent to a discussion of the double-resonance results are summarized as follows. The P dopants have a long spin-echo-decay time $T_2 = 1.1$ msec. From this plus the fact that T_2 is dominated by P-P interactions, it can be concluded that the P resides in regions of the sample where the H is dilute. For the B singly doped samples, all of the B signal occurs in moderately broad or very broad lines. These quadrupole-interaction-broadened lines can be identified as due to the threefold coordinated boron with differing local distortions. In the compensated sample, there is an additional very narrow line containing about 25% of the B, or 0.5 at. %, that we attribute to fourfold coordinated boron atoms. But for this compensated sample, about half of the B have a P near neighbor. So these four-fold coordinated B atoms, only observed in the compensated material, may consist of B with three Si and one P, i.e., $BPSi_3$ units.

The essential SEDOR results are summarized in Table II. The B-P results for the compensated sample indicate that B-P clustering occurs for about 40% of the boron. The fact that this is well beyond the random value of 8% indicates that B and P have a chemical affinity for each other in *a*-Si, a result which is substantiated by reports that B and P dopant concentrations in compensated films tend to equalize during growth even if the dopant-gas concentrations in the plasma are quite different.[38] Also the fact that the B and P tend to cluster has implications for the band structure and may give rise to neutral donor states above the valence band that are observed in compensated material.[37-39]

From this SEDOR data, we may also expect to see a heteronuclear broadening component of the P resonance comparable to the measured B-P SEDOR coupling of

$$(\Delta\omega_1^2)^{1/2}2\pi\approx 0.8\text{ kHz}\ ,$$

or, equivalently, $T_{2_{(B-P)}}\approx 200\ \mu\text{sec}$. This interaction should manifest itself as a short-time component of 200 μsec in the P echo decay for 40% of the P signal, the fraction of the P that are strongly coupled to the B. There is no indication of such a short decay in the 1.1 msec P-echo decay.[10] However, this shorter decay would only be observable if those boron nuclei which are near the phosphorus are also strongly coupled to the other boron atoms, that is, only if

$$1/T_{2_{(B-B)}}\geq 1/T_{2_{(B-P)}}\ .$$

But, the B is very dilute and experiences a large quadrupole interaction which tends to decouple the B dipolar interaction. This quadrupolar decoupling essentially makes $1/T_{2_{(B-B)}}$, already small due to the dilution, even smaller. In such a case, the B-P coupling does not contribute to the P echo decay. This is because the Hamiltonian that describes this couplilng ($\delta\omega_d I_z J_z$) commutes with the rest of the Hamiltonian describing the other interactions. It then cancels out of the expression for the echo signal.[40] When the B-B dipolar coupling is substantial, the B-P coupling does not commute with the rest of the Hamiltonian and, as a result, does not drop out of the expression for the P-echo decay. This is not the case here due to the quadrupole interaction and the large B-B separation.

Second, examine the P-H results for both the compensated and singly doped *n*-type samples. A distance of 2.6 Å for both samples is too large to be attributed to direct P—H bonding which is typically 1.4 Å, similar to that of Si—H. Neither the random nor the clustered case applies to P-H. One possible interpretation of these results is that the hydrogen is back-bonded to a Si nearest neighbor to a P. However, the determined P—H distance of 2.6 Å would require an H-Si-P angle that is much smaller than the tetrahedral angle. This structural arrangement is shown schematically in Fig. 7.

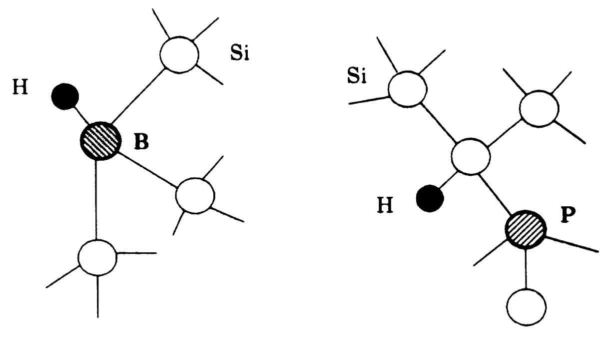

FIG. 7. Schematic of the local bonding configurations for about half the dopant sites that have hydrogen near neighbors in the singly doped samples. For B the H is a first neighbor, whereas for P the H is a second neighbor.

This structure is similar to a proposal for passivated *n*-type crystalline silicon.[7,8] For this crystalline case, it is found that the total-energy-minimum position for H is at the antibonding site of a Si nearest neighbor for a substituional P atom. The direct bonding of H to a P has a significantly higher total energy than the bonding to a neighboring Si. The detailed structure of this model, however, is different from that of Fig. 7 in that it has the H in the Si antibonding site opposite the P atom. This neighboring Si is bonded to three other Si's, the P, and the H. With the H in this antibonding site, it is significantly further from the P than for our model in Fig. 7. The calculations found that the other three antibonding sites that are closest to the P are less favorable than this further site. The amorphous case, however, has significantly more H, and the bulk of this H provides the fourth bond to a Si that is threefold coordinated to other Si. It ties up the Si dangling bond and is not thought to provide a fifth bond to the Si. As a result, Fig. 7 is not unreasonable for *a*-Si. The main point here, however, is that the model for the crystalline case has the H bonded to a Si neighbor to the P and not directly to the P, just as our model for amorphous Si.

From our SEDOR data, we may also expect to see a heteronuclear dipolar broadening component of the P resonance comparable to the measured P-H SEDOR coupling of

$$(\Delta\omega_1^2)^{1/2}2\pi\approx 1.2\text{ kHz}\ ,$$

or, equivalently, $T_{2_{(P-H)}}\approx 130\ \mu\text{sec}$. However, as for the B-P case discussed earlier, this broadening would be observable only if those hydrogen nuclei which are in close association with phosphorus are also strongly coupled to other hydrogen atoms, that is, only if

$$1/T_{2_{(\mathrm{H-H})}} \geq 1/T_{2_{(\mathrm{P-H})}} .$$

This should be the case since the T_2 of the narow hydrogen line is shorter (≈ 100 μsec) than the P-H coupling (≈ 130 μsec). This interaction should manifest itself as a short-time component consisting of about 50% of the P echo with decay constant of 130 μsec. There is no indication of such a short decay in the P-echo decay.[10] These factors imply that the hydrogen that is closely associated with phosphorus nuclei (as indicated in the P-H SEDOR data) must be isolated from the general H-spin reservoir such that

$$1/T_{2_{(\mathrm{H-H})}} \ll 1/T_{2_{(\mathrm{P-H})}} .$$

In such a case, the P-H coupling does not contribute to the P echo decay. When the H-H coupling is turned on, then the P-H coupling no longer drops out of the problem and does contribute to the P-echo decay. These facts led us to search for such a narrow hydrogen resonance line due to this H that is only coupled to neighboring P and decoupled for the other H. None was found, due most likely to the fact that, if present, it is masked by the line broadening from a distribution in chemical shifts. Nevertheless, these results support the ideas mentioned earlier that the P atoms probably reside in the dilute H phase and not in the clustered H phase.

Third, examine the B-H results. The data for the *p*-type material indicates that 40% of the B atoms have a hydrogen atom near neighbor located at a distance of 1.6 Å. This is relatively close to the B-H bonding distance found in B_2H_6 (1.4 Å) and in good agreement with a theoretically derived B-H distance (1.63 Å) in crystalline Si (Ref. 4). Thus the data would indicate that 40% of the B atoms have a hydrogen atom as a near neighbor, shown schematically in Fig. 7. This 40% is very close to the random value. In contrast, the data for the compensated material indicate that there is no short B-H distance and neither the random nor clustered case apply. Possibly the clustering of the B and P in the compensated material prevents significant B-H bonding.

This structure is very close to proposals for the B-H structure in passivated *p*-type crystalline silicon.[4,7] For this crystalline case, it is found that the total-energy-minimum corresponds to the hydrogen residing in a relaxed interstitial site between the boron and a Si neighbor. This provides a B-H distance of 1.63 Å in good agreement with our 1.6 Å. The antibonding sites of B and of Si were found to have a higher total energy. Unlike the P-H local structure, the H is a first neighbor to the B.

VI. SUMMARY

The distance between dopants and hydrogen in compensated and singly doped *a*-Si has been determined using NMR spin-echo double resonance. This is an NMR technique that is sensitive to the relative spatial relation of a selected pair of atoms. It is found that there is a nonrandom local configuration around the dopants in these materials. In the compensated samples, about half of the boron atoms have a phosphorus in the first-neighbor shell. This is much higher than the random value of 8% and indicates that there is substantial clustering of the dopants in compensated material. In addition, the location of hydrogen relative to the dopants has been studied. The hydrogen is not directly bonded to the dopants in the compensated material. This implies that the H has a higher chemical affinity for Si than for B and P or that the cluster modifies the H bonding in compensated *a*-Si. For singly doped *a*-Si, the H-dopant structure is similar for the P-doped samples but different for the B-doped material. For the B-doped case, one-quarter to one-half of the B atoms have a H in the first-neighbor shell at 1.6 Å. This is to be contrasted with the P-doped samples which have no H at this short distance. The H atoms are second or further neighbors to the P atoms and are, at their closest distance, back-bonded to a Si first neighbor to a P. This structure and, particularly, the dramatic difference between B and P in *a*-Si is similar to that proposed for hydrogen-passivated crystalline Si doped with P or B.

ACKNOWLEDGMENTS

We would like to thank C. C. Tsai for supplying the *a*-Si samples used in this study, J. A. Reimer for helpful discussions, and the Solar Energy Research Institute for support.

---

[1] See, for example, the reviews in *The Physics of Hydrogenated Amorphous Silicon,* edited by J. D. Joannopoulos and G. Lucovsky (Springer-Verlag, New York, 1984).

[2] J. C. Knights, T. M. Hayes, and J. C. Mikkelsen, Jr., Phys. Rev. Lett. **39**, 712 (1977).

[3] J. I. Pankove, D. E. Carlson, J. E. Berkreyheiser, and R. O. Wance, Phys. Rev. Lett. **51**, 2224 (1983).

[4] G. G. DeLeo and W. B. Fowler, Phys. Rev. B **31**, 6861 (1985).

[5] M. Stutzmann, Phys. Rev. B **35**, 5921 (1987).

[6] A. D. Marwick, G. S. Oehrlein, and N. M. Johnson, Phys. Rev. B **36**, 4539 (1987).

[7] K. J. Chang and D. J. Chadi, Phys. Rev. Lett. **60**, 1422 (1988).

[8] N. M. Johnson, C. Herring, and D. J. Chadi, Phys. Rev. Lett. **56**, 769 (1986).

[9] J. B. Boyce and S. E. Ready, J. Non-Cryst. Solids **97&98**, 345 (1987); S. E. Ready, J. B. Boyce, and C. Tsai, *Stability of Amorphous Silicon Alloy Materials and Devices,* Proceedings of an International Conference on Stability of Amorphous Silicon Alloy Materials and Devices, AIP Conf. No. 157, edited by B. L. Stafford and E. Sabisky (AIP, New York, 1987); MRS Conf. Proc. **95**, 153 (1987).

[10] J. B. Boyce and S. E. Ready, in *Advances in Amorphous Semiconductors,* edited by H. Fritzsche (World Scientific, Singapore, to be published).

[11] S. G. Greenbaum, W. E. Carlos, and P. C. Taylor, Solid State Commun. **43**, 663 (1982).

[12] S. G. Greenbaum, W. E. Carlos, and P. C. Taylor, J. Appl. Phys. **56**, 1874 (1984).

[13] J. A. Reimer and T. M. Duncan, Phys. Rev. B **27**, 4895 (1983).

[14] M. J. McCarthy and J. A. Reimer, Phys. Rev. B **36**, 4525 (1987).

[15] D. E. Kaplan and E. L. Hahn, J. Phys. Radium **19**, 821 (1958); M. Emshwiller, E. L. Hahn, and D. Kaplan, Phys. Rev. **118**, 414 (1960).

[16] C. P. Slichter, *Principles of Nuclear Magnetic Resonance* (Springer-Verlag, New York, 1978), p. 233.

[17] E. L. Hahn, Phys. Rev. **80**, 580 (1950).

[18] P.-K. Wang, C. P. Slichter, and J. H. Sinfelt, J. Phys. Chem. **89**, 3606 (1985).

[19] J. A. Reimer, R. W. Vaughan, and J. C. Knights, Phys. Rev. Lett. **44**, 193 (1980); Phys. Rev. B **24**, 3360 (1981).

[20] J. A. Reimer, R. W. Vaughan, and J. C. Knights, Phys. Rev. B **23**, 2567 (1981).

[21] W. E. Carlos and P. C. Taylor, Phys. Rev. B **26**, 3605 (1982).

[22] P. C. Taylor, in *Semiconductors and Semimetals* (Academic, New York, 1984), Vol. 21, Chap. 3.

[23] J. Baum, K. K. Gleason, A. Pines, A. N. Garroway, and J. A. Reimer, Phys. Rev. Lett. **56**, 1377 (1986).

[24] K. K. Gleason, M. A. Petrich, and J. A. Reimer, Phys. Rev. B **36**, 3259 (1987).

[25] M. S. Conradi and R. E. Norberg, Phys. Rev. B **24**, 2285 (1981).

[26] W. E. Carlos and P. C. Taylor, Phys. Rev. B **25**, 1435 (1982).

[27] D. J. Leopold, J. B. Boyce, P. A. Fedders, and R. E. Norberg, Phys. Rev. B **26**, 6053 (1982).

[28] P. C. Taylor, J. Non-Cryst. Solids **59&60**, 109 (1983).

[29] J. B. Boyce, M. Stutzmann, and S. E. Ready, Phys. Rev. B **32**, 6062 (1985).

[30] J. B. Boyce and M. Stutzmann, Phys. Rev. Lett. **54**, 562 (1985).

[31] J. B. Boyce, M. Stutzmann, and S. E. Ready, J. Non-Cryst. Solids **77&78**, 265 (1985).

[32] A. Abragam, *Principles of Nuclear Magnetism* (Oxford University Press, London, 1961).

[33] W. E. Carlos and P. C. Taylor, Phys. Rev. Lett. **45**, 358 (1980).

[34] G. E. Jellison, Jr. and S. G. Bishop, Phys. Rev. B **19**, 6418 (1979).

[35] P. J. Bray, J. Non-Cryst. Solids **95**, 43 (1987).

[36] C. G. Brown and D. F. Holcomb, Phys. Rev. B **10**, 3394 (1974).

[37] M. Stutzmann, D. K. Biegelsen, and R. A. Street, Phys. Rev. B **35**, 5666 (1987).

[38] R. A. Street, D. K. Biegelsen, and J. C. Knights, Phys. Rev. B **24**, 969 (1981).

[39] J. M. Marshall, R. A. Street, and M. J. Thompson, Phys. Rev. B **29**, 2331 (1987).

[40] See Ref. 32, pp. 497–501.